

## ORIGINAL ARTICLE

# Hybrid-type stretchable interconnects with double-layered liquid metal-on-polyimide serpentine structure

Doo Ri Yim<sup>1,2</sup> | Chan Woo Park<sup>1,2</sup> 

<sup>1</sup>Flexible Electronics Research Section, Electronics and Telecommunications Research Institute, Daejeon, Republic of Korea

<sup>2</sup>ETRI School (ICT-Advanced Device Technology), University of Science and Technology, Daejeon, Republic of Korea

## Correspondence

Chan Woo Park, Flexible Electronics Research Section, Electronics and Telecommunications Research Institute, Daejeon, Republic of Korea.  
Email: chanwoo@etri.re.kr

## Funding information

Institute for Information and Communications Technology Promotion, (Grant/Award Number: 2017-0-00048; Development of Core Technologies for Tactile Input/Output Panels in Skintronics [Skin Electronics])

## Abstract

We demonstrate a new double-layer structure for stretchable interconnects, where the top surface of a serpentine polyimide support is coated with a thin eutectic gallium–indium liquid metal layer. Because the liquid metal layer is constantly fixed on the solid serpentine body in this liquid-on-solid structure, the overall stretching is accomplished by widening the solid frame itself, with little variation in the total length and cross-sectional area of the current path. Therefore, we can achieve both invariant resistance and infinite fatigue life by combining the stretchable configuration of the underlying body with the freely deformable nature of the top liquid conductor. Further, we fabricated various types of double-layer interconnects as narrow as 10  $\mu\text{m}$  using the roll-painting and lift-off patterning technique based on conventional photolithography and quantitatively validated their beneficial properties. The new interconnecting structure is expected to be widely used in applications requiring high-performance and high-density stretchable circuits owing to its superior reliability and capability to be monolithically integrated with thin-film devices.

## KEYWORDS

double-layer, EGaIn, liquid metal, serpentine, stretchable interconnect

## 1 | INTRODUCTION

In many approaches for fabricating stretchable electronic circuits [1–6], the overall stretchability is provided by stretchable interconnecting regions, while active devices vulnerable to even a small amount of mechanical deformation, such as thin-film transistors [1,2], sensors [3,4], or light-emitting devices [5,6], are located within rigid islands. For achieving stretchable interconnects, various strategies have been employed [7–14]. For example, non-stretchable metal thin films can be configured as stretchable shapes such as serpentine [7,8], wavy [9,10], or coiled structures [11], which can accommodate the

tensile strain via structural transformation. It is also possible to use intrinsically stretchable conductors as interconnecting materials, where metal or carbon-based conductive fillers are dispersed within an elastomeric matrix [12–14].

However, for an integrated circuit to function properly under stretching, it is not enough to maintain the electrical connection among device elements, but the resistance of interconnects must also remain nearly constant irrespective of the strain. Unfortunately, it is difficult to simultaneously satisfy these two conditions. For example, interconnects made by stretchable composite conductors have large elongation and high durability

under repetitive deformation, but their resistance changes significantly with the variation in dimension induced by the deformation [13–15]. It is also difficult to achieve high conductivity and narrow pattern widths comparable with thin metal films because the conductive fillers are dispersed within a highly viscous elastomeric matrix [1,12–15]. However, thin metal interconnects with serpentine shapes exhibit little variation in resistance even under a large amount of stretching, because the total length of the conducting path is not affected by the elastic widening of the entire structure [8,16]. They can also be monolithically integrated with thin-film devices, which are fabricated using conventional photolithography and etching techniques [7,17]. However, the mechanical reliability against repeated stretching is limited in this case, because the local stress concentration at the serpentine structure's angular points inevitably results in fatigue failure [18,19].

Recently, as an alternative candidate for stretchable conductors, eutectic gallium-based liquid alloys have been investigated extensively [20–25]. As a low-viscosity and highly conductive fluid [20], the liquid metal can provide extreme stretchability without mechanical degradation, as well as low resistance similarly to solid metals [21,22]. We demonstrated in our earlier works [23–25] that the liquid metal can be patterned by a roll-painting and lift-off technique based on photolithography, making it possible to monolithically integrate narrow liquid metal interconnects with thin-film transistors. However, as the liquid metal channel's geometry is affected by

the deformation of the surrounding elastomer matrices, the variation of resistance with strain remains unavoidable [21–23].

In this study, we provide a new double-layer structure for stretchable interconnects, where the serpentine polyimide support's top surface is coated with a thin liquid metal layer. The variation in the length or cross-sectional area of the current path is minimal with this structure because stretching is achieved by widening the solid frame while the liquid metal layer remains constant. We can obtain stretchable interconnects where the resistance remains nearly constant, but no fatigue failure occurs under repeated stretching by combining the stretchable configuration of the underlying body and the freely deformable nature of the top liquid metal. We characterized such beneficial properties quantitatively, by comparing the stretching behavior of the new liquid-on-solid structure with those of the solid-on-solid and liquid-only serpentine interconnects.

## 2 | EXPERIMENTAL

### 2.1 | Fabrication of hybrid liquid-on-solid serpentine interconnects

Figure 1A,B demonstrates the structure and fabrication process of the hybrid liquid-on-solid serpentine interconnect, respectively. First, a polyimide layer (about 4  $\mu\text{m}$ ) was spin-coated on a glass wafer and cured, on which

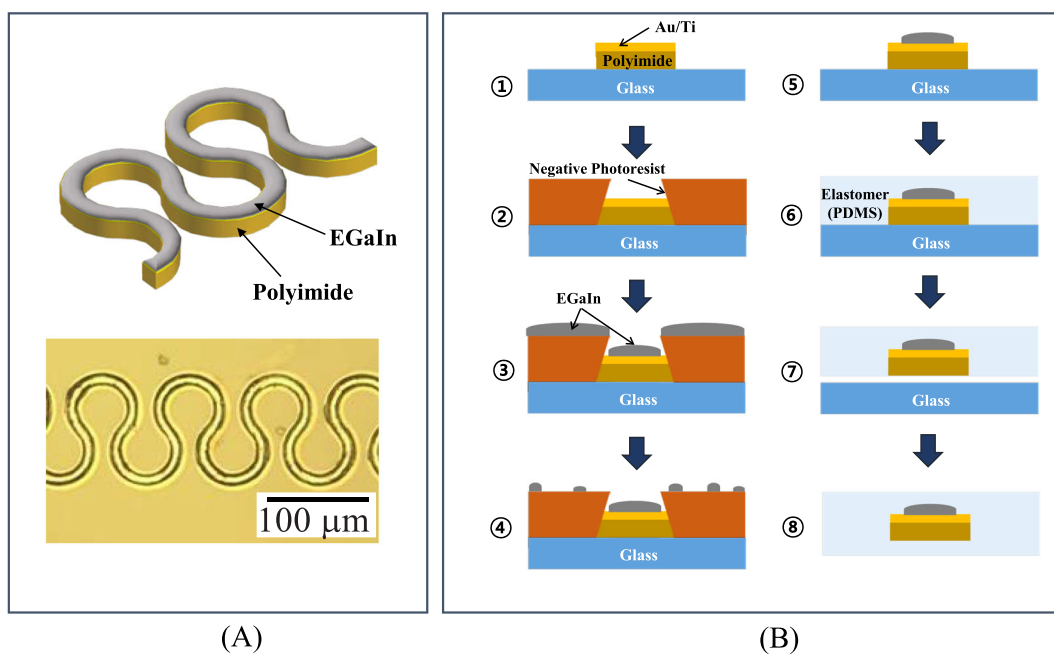


**FIGURE 1** Schematic illustrations of the (A) structure and (B) fabrication process of the hybrid liquid-on-solid serpentine interconnects

serpentine Au/Ti (80 nm/20 nm) patterns were formed using electron-beam evaporation and lift-off techniques. The underlying polyimide layer was dry-etched with oxygen plasma (Step 1) using the Au/Ti layer as an etch mask. Further, a negative photoresist with an approximately 5- $\mu\text{m}$  thickness was spin-coated, and patterns with negative-sloped sidewalls were formed by photolithography, such that only the top surface of polyimide bodies was exposed (Step 2). A eutectic gallium–indium (EGaIn) liquid alloy composed of 75.5% Ga and 24.5% In by weight was dropped on the substrate and evenly spread using a hand-roller (Step 3) after oxygen plasma treatment on the Au surface, which functions as an adhesive layer. After the entire exposed Au area was filled with the liquid metal, a small amount of water was dropped and wiped with the hand-roller by which most of the excessive EGaIn within the photoresist region was removed (Step 4). The EGaIn/photoresist layer was lifted off by immersing the sample in acetone, leaving behind the double-layer (EGaIn/polyimide) interconnects (Step 5). Next, after casting a 10:1 mixture (weight ratio) of a polydimethylsiloxane (PDMS) prepolymer and curing agent on the substrate (Step 6), the entire structure was released from the glass substrate by the laser-lift-off technique using a XeCl excimer laser (305 nm) (Step 7). Finally, a backside capping PDMS layer was cast with the same thickness as that of the top PDMS layer (about 500  $\mu\text{m}$ ) (Step 8).

## 2.2 | Fabrication of the solid-on-solid and liquid-only serpentine interconnects

By modifying the fabrication process of the hybrid interconnect, Figure 1 shows that the solid-on-solid and

liquid-only interconnects were also produced as control groups. Figure 2A shows that the solid-on-solid structure was obtained immediately after dry etching the polyimide layer using the top serpentine Au/Ti pattern as an etch mask (as Step 1 in Figure 1), which was then transferred to the PDMS substrate without forming the top liquid metal layer. The serpentine EGaIn/Au/Ti patterns were first produced on the polyimide-coated glass substrate, and the top PDMS layer was cast to produce the liquid-only interconnects. Further, the polyimide layer was removed by dry etching before casting the backside capping PDMS layer after releasing the entire structures from the glass substrate, as demonstrated in Figure 2B.

## 3 | RESULTS AND DISCUSSION

Figure 3 shows the layout of some test devices in an array within a 100 mm  $\times$  100 mm area, where eight types of serpentine interconnect with different geometric parameters are included. Figure 3 shows that the width of top EGaIn lines was 10  $\mu\text{m}$  or 20  $\mu\text{m}$ , whereas the underlying polyimide body was two times wider. For each line-width value, the arc radius was also varied in the ranges of 30  $\mu\text{m}$  to 60  $\mu\text{m}$  and 60  $\mu\text{m}$  to 120  $\mu\text{m}$ .

It was nearly impossible to produce straight lines narrower than 20  $\mu\text{m}$  in previous works based on the roll-painting and lift-off technique for EGaIn [23–25] owing to local agglomeration or uneven EGaIn fluid wetting. It is more difficult to obtain fine and resolved pattern shapes for serpentine structure because closely spaced line segments readily agglomerate. Thus, the roll-painting process has been modified to overcome such limitations in this study. Figure 4 shows that after

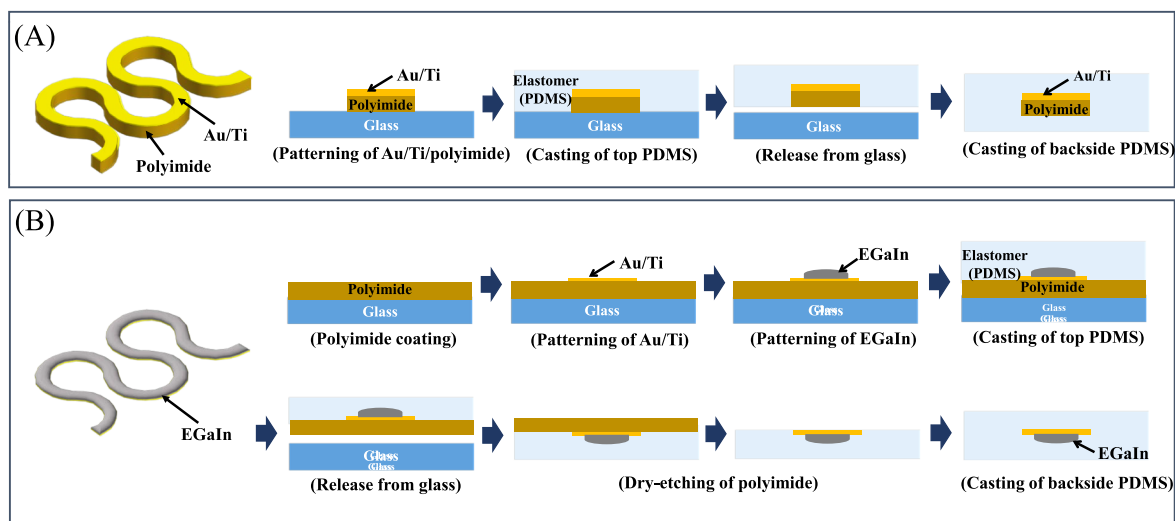
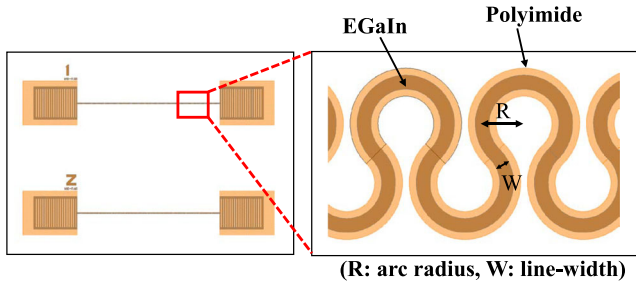


FIGURE 2 Schematic illustration of the structure and fabrication process of (A) solid-on-solid and (B) liquid-only serpentine interconnects



(R: arc radius, W: line-width)

Line-width (EGaIn/Polyimide)	Arc Radius (EGaIn)
10 μm / 20 μm	30 μm, 40 μm, 50 μm, 60 μm
20 μm / 40 μm	60 μm, 80 μm, 100 μm, 120 μm

FIGURE 3 Mask layout and design parameters for eight types of serpentine structures

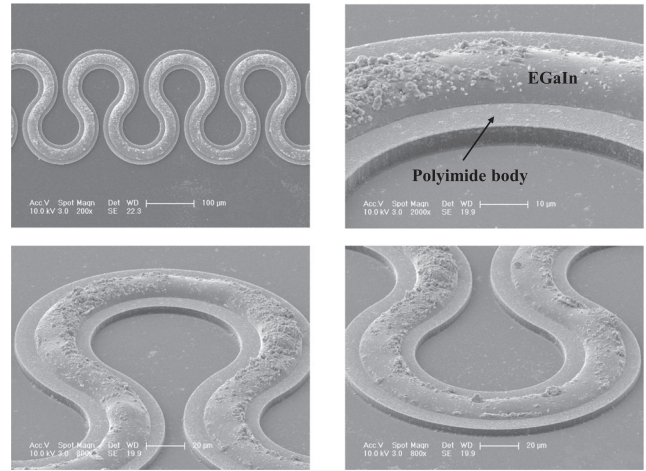


FIGURE 5 Scanning electron microscopy images of liquid-on-solid serpentine interconnects as fabricated on the glass wafer

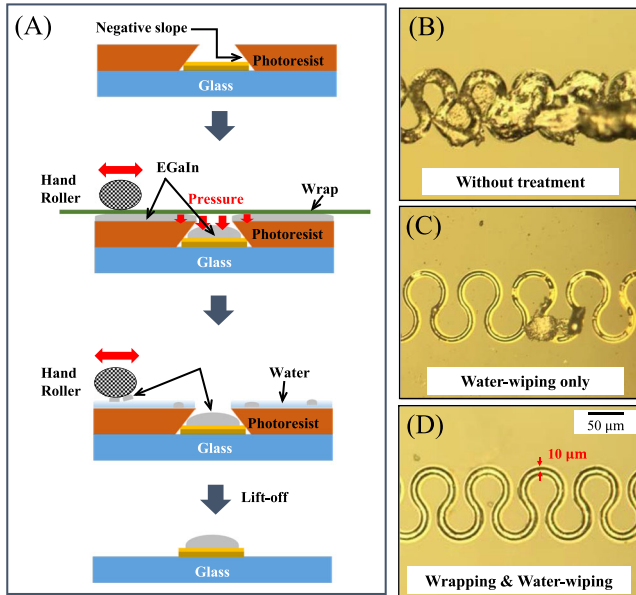


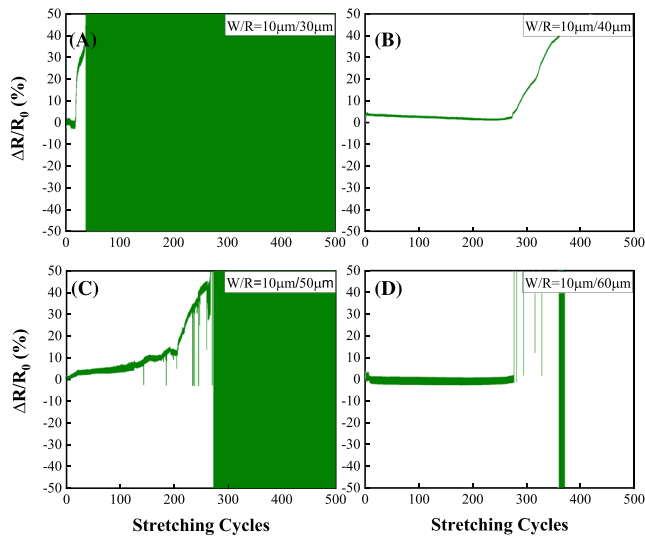
FIGURE 4 (A) Schematic illustration of the modified roll-painting and lift-off technique and the pattern shapes obtained by (A) no treatment, (B) water-wiping only, and (C) both wrapping and water-wiping

dropping EGaIn on the photoresist layer and before rolling, the entire specimen was covered with a plastic wrap to confine the liquid metal during rolling and efficiently push it into concave patterns. Most EGaIn over the photoresist area could be removed before lift-off in acetone after the painting process by dropping a small amount of water and wiping the surface with the roller intensively. The quality of serpentine EGaIn patterns was significantly improved by introducing those two additional steps (Figure 4B, C, and D).

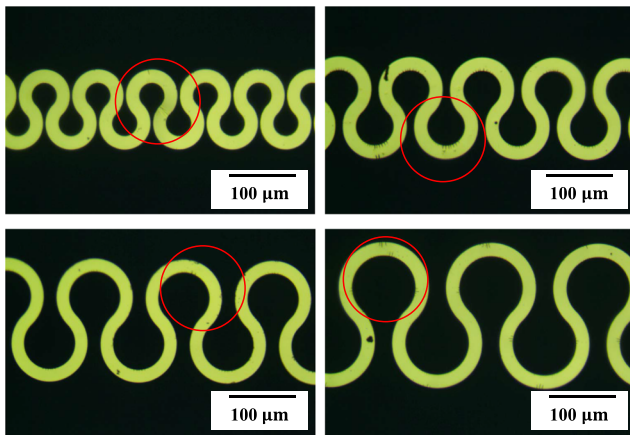
Row	Width/Radius (μm)	Resistance (kΩ)
Row 1	10/30	0.71% ± 6.50%
Row 2	10/40	0.72% ± 7.00%
Row 3	10/50	0.69% ± 9.70%
Row 4	10/60	0.62% ± 6.60%
Row 5	20/60	0.19% ± 0.50%
Row 6	20/80	0.21% ± 1.60%
Row 7	20/100	0.19% ± 1.60%
Row 8	20/120	0.21% ± 2.50%

FIGURE 6 Representative average values and deviation of electrical resistance for liquid-on-solid serpentine interconnects with varying dimension across a 100 mm × 100 mm area

Figure 5 shows representative scanning electron microscopy (SEM) images of the liquid-on-solid serpentine interconnect, as fabricated on a glass substrate. Although several previous approaches have been demonstrated to be successful in patterning EGaIn [20,26], it remains difficult to simultaneously achieve fine feature sizes (tens of micrometers) and precise alignment (within a few micrometers) [27–30]. However, the modified roll-painting and lift-off technique, which is based on conventional photolithography, can provide a well-aligned double-layer structure with smooth line edges and a rounded surface on the top EGaIn layer. Gallium-based liquid alloys, unlike ordinary liquid fluids, form a thin oxide skin in air, which mechanically stabilizes even irregular surface profiles instantly [20]. Figure 5 shows that several particle-like protrusions were formed on the liquid metal surface, which is thought to be due to dynamic contact between the liquid metal and roller head during the roll-painting process.



**FIGURE 7** Representative variation of the resistance of solid-on-solid serpentine interconnects under cyclic stretching of 30%, for arc radii of (A) 30  $\mu\text{m}$ , (B) 40  $\mu\text{m}$ , (C) 50  $\mu\text{m}$ , and (D) 60  $\mu\text{m}$  at the line width of 10  $\mu\text{m}$  (stretching rate: 15 mm/min)



**FIGURE 8** Optical microscopy images of microcracks on solid-on-solid serpentine interconnects failed during the cyclic stretching

We demonstrated in our earlier work [23] that the height of EGaIn patterns is similar to the photoresist layer's thickness, as long as the rolling pressure is high enough to push EGaIn down to the bottom of trenches within the photoresist layer. The variation in height and width was measured to be less than 10% along 30-mm-long straight traces [23]. In this study, we could confirm the uniformity of serpentine patterns by measuring the electrical resistance of interconnects across a 100 mm  $\times$  100 mm area. The deviation in the resistance was measured to be less than 10% for each type of serpentine structure located within the area (Figure 6).

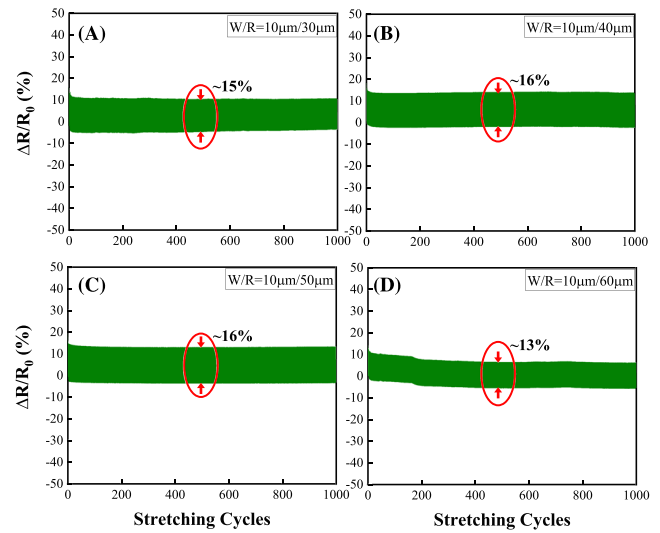


**FIGURE 9** Representative variation of the resistance of liquid-only serpentine interconnects under cyclic stretching of 30%, for arc radii of (A) 30  $\mu\text{m}$ , (B) 40  $\mu\text{m}$ , (C) 50  $\mu\text{m}$ , and (D) 60  $\mu\text{m}$  at the line width of 10  $\mu\text{m}$  (stretching rate: 15 mm/min)

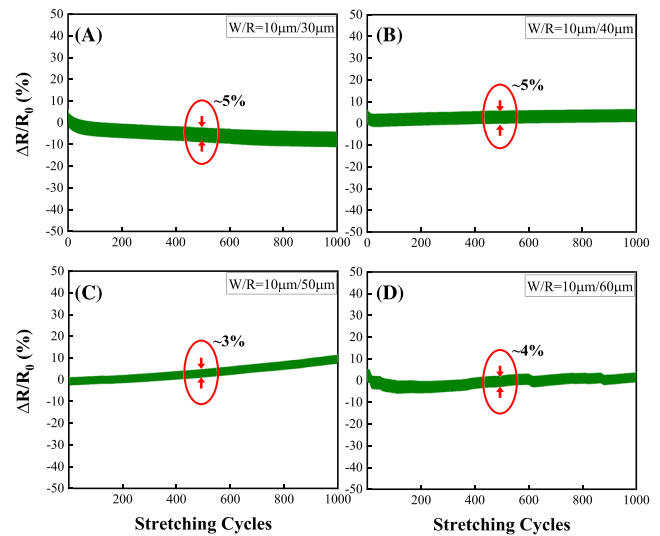


**FIGURE 10** Representative variation of the resistance of liquid-on-solid serpentine interconnects under cyclic stretching of 30%, for arc radii of (A) 30  $\mu\text{m}$ , (B) 40  $\mu\text{m}$ , (C) 50  $\mu\text{m}$ , and (D) 60  $\mu\text{m}$  at the line width of 10  $\mu\text{m}$  (stretching rate: 15 mm/min)

We first investigated the stretching behavior of the solid-on-solid and liquid-only serpentine interconnects with the same geometry to quantitatively examine the beneficial properties of the hybrid liquid-on-solid structure. Figure 7 shows the resistance variation of the solid-on-solid structure under 30% cyclic stretching. In this case, the resistance was kept almost constant (within the variation of 1% to 2%) throughout the initial cycles, but



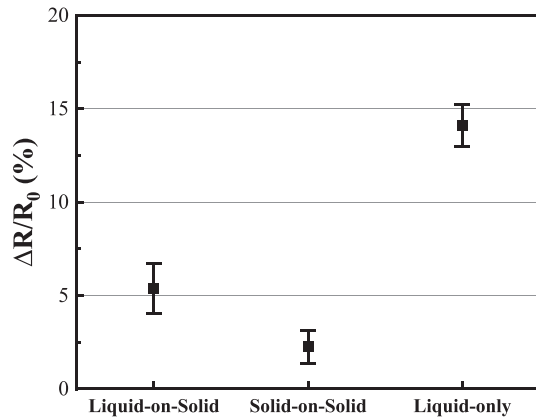


**FIGURE 11** Variation of the normalized electrical resistance under cyclic stretching of 30%, for liquid-on-solid and liquid-only (500 cycles), and solid-on-solid (20 cycles) interconnects. Each data point was obtained by averaging those values from eight different devices

as the stretching progressed, most interconnects showed a sudden increase in resistance, resulting in their eventual failure. We discovered many microcracks after the failure (Figure 8). The high asymmetry of the layer structure is considered responsible for the solid-on-solid structure's poor durability because the thin metal layer far from the neutral mechanical plane undergoes intensive stress under stretched conditions [31]. As demonstrated in previous works [7,8,32], the stability of solid-on-solid interconnects can be significantly enhanced by adding a top polyimide layer, such that the metal film can be located within the central plane between two identical supports. However, even with such structural optimization retarding effects, all kinds of thin solid metal would eventually fracture under prolonged repeated deformation [8,18,19,32].

The liquid-only interconnect, unlike the solid-on-solid structure, can provide extremely high stability under repeated stretching. Figure 9 shows that the electrical connectivity of the liquid-only interconnect was stable without any abrupt increase in resistance or breaking during 1000 cycles of 30% stretching. A volume of a liquid metal contained within an elastomer can be freely reformed to accommodate any type of external strain and can provide infinite resistance to the fatigue failure as long as the elastomer matrix is maintained. Thus, the use of liquid metal may be the ultimate solution for preventing stretchable interconnects from degrading mechanically.

However, the resistance across a liquid metal channel is significantly influenced by external strain, as the total length and cross-sectional area vary accordingly [21–23]. Various types of pressure or strain sensors using liquid metal have been reported extensively based on such properties [33–36]. Figure 9 shows that the liquid-only serpentine interconnect also exhibited resistance

variation of about 15% under 30% stretching, which is much larger than those of undamaged solid-on-solid interconnects in Figure 7.

It is necessary to minimize the resistance variation in response to strain and maintain the electric connectivity when using any stretchable interconnects in circuits requiring precise control, such as multifunctional displays [37] or analog sensor arrays [38]. For example, in wearable systems for human motion monitoring, piezo-resistive sensors are often used in measuring the movement of certain joints or muscles [39]. If the resistance of interconnects transmitting the sensor signal is also sensitive to human motion, it would be difficult to precisely analyze the collected data. In this scenario, the application of the liquid-only interconnect is limited.

Considering the complementary characteristics of solid-on-solid and liquid-only interconnects observed under repeated stretching, combining the advantages of each structure and achieving the invariant resistance and quasi-infinite fatigue life simultaneously would be ideal. In this study, we demonstrated that the new hybrid liquid-on-solid structure can satisfy such requirements by preventing the liquid metal layer's dimensional change even under stretched conditions. We could minimize the resistance variation to as low as 5% under 30% stretching with this structure (Figure 10) while maintaining similar mechanical stability under cyclic stretching as the liquid-only interconnects.

In the case of liquid-only interconnects embedded within an elastomer, a liquid metal channel adapts to the stretched matrix by extending the overall channel length and reducing the cross-sectional area. However, in the liquid-on-solid structure, the liquid metal layer is fixed on a rigid serpentine body whose length is kept constant during stretching. Therefore, the liquid-on-solid serpentine interconnect can provide a much smaller resistance variation than can the liquid-only structure (Figure 11) because it is being stretched mainly by widening or twisting the solid frame itself.

Figure 11 shows that the resistance variation of liquid-on-solid interconnects is still slightly larger than that of the solid-on-solid structure. Such a difference is thought to be due to the local fluctuation in the liquid metal layer's cross-sectional area, induced by limited deformation from the top side of the liquid metal in contact with the soft elastomer. However, the electrical resistance of liquid-on-solid interconnects was 30% to 40% that of solid-on-solid interconnects for the same serpentine structure dimension. Therefore, although the relative resistance variation ( $\Delta R/R_0$ ) of liquid-on-solid interconnects under stretching was about two times larger than that of solid-on-solid structures (Figure 11), the absolute resistance variation ( $\Delta R$ ) was almost the same. Thus, the benefits of the hybrid

structure, which provides both the small resistance variation and high reliability, are obvious.

Previously, most studies employing EGaIn interconnects have focused on manual integration with bulky and discrete device chips [28,40,41] because it is difficult to achieve precise alignment between the EGaIn interconnects and devices at the micrometer scale. However, using the roll-painting and lift-off technique, which enables precise patterning of the liquid metal, we can apply the new interconnecting structure for monolithically integrated high-density sensor or TFT circuits, providing higher performance.

## 4 | CONCLUSION

We have demonstrated a new hybrid-type stretchable interconnects, in which a thin gallium-based liquid metal layer is located on the top surface of the serpentine polyimide support. The liquid metal lines may be integrated monolithically on the solid support in a well-aligned manner using the roll-painting and lift-off technique based on conventional photolithography. In this double-layer structure, the liquid metal conductor provides extremely high resistance to the fatigue failure, whereas the resistance variation can be avoided as stretching is performed by widening the solid frame. The new interconnecting structure could be widely used in applications requiring high-density and high-complexity stretchable circuits by simultaneously satisfying those key properties for stretchable interconnects.

## ACKNOWLEDGMENTS

This work was supported by Institute for Information and Communications Technology Promotion (IITP) grant funded by the Korea government (MSIT) (Grant No. 2017-0-00048, Development of Core Technologies for Tactile Input/Output Panels in Skintronics [Skin Electronics]).

## CONFLICTS OF INTEREST

The authors declare that there are no conflicts of interest.

## ORCID

Chan Woo Park  <https://orcid.org/0000-0002-8666-016X>

## REFERENCES

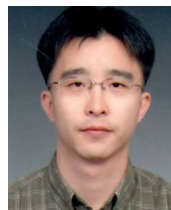
- N. Matsuhisa et al., *Printable elastic conductors with a high conductivity for electronic textile applications*, Nat. Commun. **6** (2015), 7461.
- J.-S. Choi et al., *Stretchable organic thin-film transistors fabricated on wavy-dimensional elastomer substrates using stiff-island structures*, IEEE Electron Device Lett. **35** (2014), no. 7, 762–764.
- Q. Hua et al., *Skin-inspired highly stretchable and conformable matrix networks for multifunctional sensing*, Nat. Comm. **9** (2018), article no. 244.
- S. Y. Hong et al., *Stretchable active matrix temperature sensor array of polyaniline nanofibers for electronic skin*, Adv. Mater. **28** (2016), no. 5, 930–935.
- J. Byun et al., *Fully printable, strain-engineered electronic wrap for customizable soft electronics*, Sci. Rep. **7** (2017), article no. 45328.
- M. Choi et al., *Stretchable active matrix inorganic light-emitting diode display enabled by overlay-aligned roll-transfer printing*, Adv. Funct. Mater. **27** (2017), no. 11, article no. 1606005.
- D.-H. Kim et al., *Ultrathin silicon circuits with strain-isolation layers and mesh layouts for high-performance electronics on fabric, vinyl, leather, and paper*, Adv. Mater. **21** (2009), no. 36, 3703–3707.
- R. Verplancke et al., *Thin-film stretchable electronics technology based on meandering interconnections: Fabrication and mechanical performance*, J. Micromech. Microeng. **22** (2012), no. 1, article no. 015002.
- C. W. Park et al., *Fabrication of well-controlled wavy metal interconnect structures on stress-free elastomeric substrates*, Microelectron. Eng. **113** (2014), 55–60.
- C. W. Park et al., *Locally-tailored structure of an elastomeric substrate for stretchable circuits*, Semicond. Sci. Technol. **31** (2016), no. 2, article no. 025013.
- C. W. Park et al., *Stretchable copper interconnects with three-dimensional coiled structures*, J. Micromech. Microeng. **23** (2013), no. 12, article no. 127002.
- T. Sekitani et al., *Stretchable active-matrix organic light-emitting diode display using printable elastic conductors*, Nat. Mater. **8** (2009), 494–499.
- T. Sekitani et al., *A rubberlike stretchable active matrix using elastic conductors*, Science **321** (2008), no. 5895, 1468–1472.
- T. Araki et al., *Printable and stretchable conductive wirings comprising silver flakes and elastomers*, IEEE Electron Device Lett. **32** (2011), no. 10, 1424–1426.
- J. Liang, K. Tong, and Q. Pei, *A water-based silver-nanowire screen-print ink for the fabrication of stretchable conductors and wearable thin-film transistors*, Adv. Mater. **28** (2016), no. 28, 5986–5996.
- K. L. Lin and K. Jain, *Design and fabrication of stretchable multilayer self-aligned interconnects for flexible electronics and large-area sensor arrays using excimer laser photoablation*, IEEE Electron Device Lett. **30** (2009), no. 1, 14–17.
- D.-H. Kim et al., *Optimized structural designs for stretchable silicon integrated circuits*, Small **5** (2009), no. 24, 2841–2847.
- D. S. Gray, J. Tien, and C. S. Chen, *High-conductivity elastomeric electronics*, Adv. Mater. **16** (2004), no. 5, 393–397.
- M. Gonzalez et al., *Design of metal interconnects for stretchable electronic circuits*, Microelectron. Reliab. **48** (2008), no. 6, 825–832.
- M. D. Dickey, *Stretchable and soft electronics using liquid metals*, Adv. Mater. **29** (2017), no. 27, article no. 1606425.
- S. Zhu et al., *Ultrastretchable fibers with metallic conductivity using a liquid metal alloy core*, Adv. Funct. Mater. **23** (2013), no. 18, 2308–2314.
- H.-J. Kim, C. Son, and B. Ziaie, *A multi-axial stretchable interconnect using liquid-alloy-filled elastomeric microchannels*, Appl. Phys. Lett. **92** (2008), article no. 011904.

23. C. W. Park et al., *Photolithography-based patterning of liquid metal interconnects for monolithically integrated stretchable circuits*, ACS Appl. Mater. Interfaces **8** (2016), no. 24, 15459–15465.
24. Y. G. Moon et al., *Freely deformable liquid metal grids and stretchable and transparent electrodes*, IEEE Trans. Electron. Devices **64** (2017), no. 12, 5157–5162.
25. C. W. Park et al., *Stretchable active matrix of oxide thin-film transistors with monolithic liquid metal interconnects*, Appl. Phys. Express **11** (2018), no. 12, article no. 126501.
26. I. D. Joshipura et al., *Methods to pattern liquid metals*, J. Mater. Chem. C **3** (2015), 3834–3841.
27. A. Tabatabai et al., *Liquid-phase gallium–indium alloy electronics with microcontact printing*, Langmuir **29** (2013), no. 20, 6194–6200.
28. Y. Zheng et al., *Personal electronics printing via tapping mode composite liquid metal ink delivery and adhesion mechanism*, Sci. Rep. **4** (2014), article no. 4588.
29. J. W. Boley et al., *Direct writing of gallium-indium alloy for stretchable electronics*, Adv. Funct. Mater. **24** (2014), no. 23, 3501–3507.
30. Y. Gao, H. Li, and J. Liu, *Direct writing of flexible electronics through room temperature liquid metal ink*, PLoS ONE **7** (2012), article no. e45485.
31. A. L. Estang-Levallois et al., *A converging route towards very high frequency, mechanically flexible, and performance stable integrated electronics*, J. Appl. Phys. **113** (2013), no. 15, article no. 153701.
32. Y.-Y. Hsu et al., *Polyimide-enhanced stretchable interconnects: design, fabrication, and characterization*, IEEE Trans. Electron. Devices **58** (2011), no. 8, 2680–2688.
33. Y.-L. Park et al., *Hyperelastic pressure sensing with a liquid-embedded elastomer*, J. Micromech. Microeng. **20** (2010), no. 12, article no. 125029.
34. Y.-L. Park, *Design and fabrication of soft artificial skin using embedded microchannels and liquid conductors*, IEEE Sen. J. **12** (2012), no. 8, 2711–2718.
35. H.-L. Yan et al., *Coaxial printing method for directly writing stretchable cable as strain sensor*, Appl. Phys. Lett. **109** (2016), no. 8, article no. 083502.
36. J. C. Yeo et al., *Triple-state liquid-based microfluidic tactile sensor with high flexibility, durability, and sensitivity*, ACS Sens. **1** (2016), no. 5, 543–551.
37. J. H. Koo et al., *Flexible and stretchable smart display: Materials, fabrication, device design, and system integration*, Adv. Funct. Mater. **28** (2018), no. 35, article no. 1801834.
38. L. Xiang et al., *Recent advances in flexible and stretchable sensing systems: From the perspective of system integration*, ACS Nano **14** (2020), no. 6, 6449–6469.
39. H. Soury et al., *Wearable and stretchable strain sensors: Materials, sensing mechanisms, and applications*, Adv. Intell. Syst. **2** (2020), no. 8, article no. 2000039.
40. S. H. Jeong et al., *Transfer atomization patterning of liquid alloys for microfluidic stretchable wireless power transfer*, Sci. Rep. **5** (2015), 8419.
41. Q. Wang et al., *Fast fabrication of flexible functional circuits based on liquid metal dual-trans printing*, Adv. Mater. **27** (2015), no. 44, 7109–7116.

## AUTHOR BIOGRAPHIES



**Doo Ri Yim** received her BS degree in Electronic Engineering from Incheon National University, Incheon, Republic of Korea, in 2016 and her MS degree in advanced device technology from ETRI School, University of Science and Technology, Daejeon, Republic of Korea, in 2019. She worked for the Process Engineering Lab, Korea Advanced Nano Fab Center, Suwon, Gyeonggi-do, Republic of Korea, from 2019 to 2020. Since 2020, she has been with the KLA Corp's PATTERNING Business Unit, Hwaseong, Gyeonggi-do, Republic of Korea, where she is now an associate engineer. Her main roles and responsibilities are image analytics and inspection for process optimization.



**Chan Woo Park** received his BS, MS, and PhD degrees in Materials Science and Engineering from Korea Advanced Institute of Science and Technology, Daejeon, Republic of Korea, in 1994, 1996, and 2000, respectively. Since 2000, he has been with the Electronics and Telecommunications Research Institute, Daejeon, Republic of Korea, where he is now a principal researcher and Director of Flexible Electronics Research Section. His main research interests comprise flexible or stretchable electronic circuits and electronic skins.

**How to cite this article:** D. R. Yim and C. W. Park, *Hybrid-type stretchable interconnects with double-layered liquid metal-on-polyimide serpentine structure*, ETRI Journal (2021), 1–8. <https://doi.org/10.4218/etrij.2021-0188>